ARTICLE

Proliferation of Epithelial Cells on PDMS Substrates with Micropillars Fabricated with Different Curvature Characteristics

C. K. M. Ng · K. N. Yu

Abstract The present work studied the proliferation of epithelial cells when they were cultivated on substrates with micropillars fabricated with the same height but with different curvature characteristics. A special micro-fabrication method was employed to produce these micropillar substrates. Polyallyldiglycol carbonate (PADC) films were first irradiated by alpha particles and then chemically etched to reach or beyond the "transition" phase to form casts with micrometer-sized pits with the same depth, but with different size and shape. Polydimethylsiloxane (PDMS) replicas of these PADC films then gave the desired substrates with micropillars with the same height but with different curvature characteristics. The micropillars on the PDMS substrates were found to be capable of changing the response of HeLa cells in terms of the percentages of cells in the S-phase and the attached cell numbers after 3-day cell culture. This demonstrated that the proliferation of the HeLa cells could be changed through mechanosensing the substrate curvature.

1 Introduction

Advances in tissue engineering and biomedical engineering require understanding of biological processes of cells on substrates or scaffolds. It is understood that cell attachment is facilitated by interactions between receptors on cell membranes and the extracellular matrix (ECM), and such interactions are well characterized in terms of cell cytoskeleton, focal adhesions and integrin involvement [1].

C. K. M. Ng · K. N. Yu (✉)
Department of Physics and Materials Science, City University of Hong Kong, Tat Chee Avenue, Kowloon Tong, Hong Kong
e-mail: peter.yu@cityu.edu.hk

Different ECM environments will provide different input signals to the cells to change their behavior such as growth, migration and differentiation. The input signals can be broadly categorized as topographical, mechanical and chemical cues. In particular, the cellular response to physical or mechanical characteristics of the ECM is referred to as ECM mechanosensing which has emerged as an important mechanism in the studies of cellular response to the ECM [2–4].

Many studies on cellular response to physical or mechanical characteristics of the ECM were carried out using pillar systems, such as cell deformation [5, 6], differentiation [5, 7, 8] and migration [9–12]. For example, mesenchymal stem cells preferentially differentiated [5] and osteosarcoma cancer cells increased their malignant transformation [6] due to the micropillar geometry. In particular, increase of pillar heights from 1 to 10 μm affected the in vitro adhesion and guide morphology of fibroblasts by laminin expression enhancement [9]. Furthermore, the spacing between 5 and 10 μm of pillars was shown to rearrange the actin cytoskeleton and governed fibroblast migration in vitro [12]. Green et al. [13] studied the growth rate of human abdomen fibroblasts cultured on substrates patterned with rectangular pit or pillar arrays, and observed that cells were more sensitive to pits or pillars with smaller size. However, different investigations on pillar-associated cellular responses sometimes gave inconsistent results, which might be in part due to the use of different cell types, culture environments and materials. For instance, cellular proliferation was not detected with some spatial arrangements of pillars but was observed with others [12, 14].

One interesting topographical cues is curvature [15]. Although studies on cellular response to curvature on pillars were relatively few, there were a number of interesting

and enlightening results in the literature demonstrating the cellular responses to substrate curvature. For example, Curtis and Varde [16] illustrated that cells probably reacted to the topographical features such as curvature. Dunn and Heath [17] found that fibroblasts responded to the substrate curvature when the latter was comparable to the cell size. Interestingly, Berry et al. [18] explicitly stated that fibroblasts had an apparent preference for entering pits with larger diameters on the substrate, and suggested that the cells might be sensitive to changes in radius of curvature of the pit walls. Furthermore, Smeal et al. [19] suggested that the substrate curvature affected the direction of nerve outgrowth, while James et al. [20] suggested that it affected the lamellipodial distribution and cell polarity. Similarly, Rumpler et al. [21] reported that tissues grew preferentially on surfaces with higher curvatures.

As such, it is pertinent and interesting to study the cellular response to the curvature of pillars. The relatively few studies on this aspect might be partially attributed to the lack of convenient methods to generate pillars with different and well-defined curvature. In the present work, we proposed a special technique to fabricate micropillars with the same height but with different curvature characteristics. Polyallyldiglycol carbonate (PADC) films were first irradiated by alpha particles and then chemically etched to reach the "transition" phase (see Sect. 2) to form casts with micrometer-sized pits with the same depth, but with different size and shape. Polydimethylsiloxane (PDMS) replicas of these irradiated and chemically etched PADC films then gave the desired substrates with micropillars with the same height but with different size and shape.

Variation in the proliferation rate of cells was an important topography effect. For example, increase in cell proliferation was observed on nanostructured poly(lactic-co-glycolic acid) (PLGA) films [22]. Rajnicek et al. [23] demonstrated that neurite growth of central nerve system neurons was increased by groove patterns. Hamilton et al. [24] discovered that discontinuous-edge surfaces altered proliferative responses from osteoblasts at early time points (<1 week). Berry et al. [25] observed an increase in the proliferation of fibroblast with decreasing pit diameter on quartz surface. Su [26] studied substrates with micropillars, which increased the number of hematopoietic stem cells. Baker et al. [27] demonstrated a substantially enhanced proliferation of fibroblasts on substrates with cylindrical pillars. In contrast, Nematollahi et al. [28] observed that epithelial cells adhered on six-sided pillar substrates exhibited reduced proliferation, while Choi et al. [29] revealed that human foreskin fibroblasts exhibited significantly lower proliferation on needle-like nanoposts. In the present work, we examined the behavior of HeLa cells on substrates with micropillars with different curvature characteristics in terms of their proliferation through the S-phase marker expression and attached cell numbers.

2 Methodology

2.1 Fabrication of Micropillar Substrates

In the present work, PADC films with a thickness of 1,000 μm (Page Mouldings (Pershore) Limited, Worcestershire) were employed to fabricate our casts for our cell-culture substrates. PADC films are commonly used solid-state nuclear track detectors [30]. PADC films were prepared with a size of 2×2 cm^2. The PADC films were divided into two groups for different treatments. The first group of films was irradiated with 5 MeV alpha particles for 30 s using an ^{241}Am alpha-particle source with an activity of 0.1151 μCi through a collimator to provide more or less normal incidence of the alpha particles. Chemical etching was then employed to form pits on these irradiated PADC film. The alpha-particle irradiation duration determined the density of the pits after chemical etching, while the etching period determined the depth, size and profile of the pits [30].

To ensure the same depth for all these pits, we chose to etch these irradiated PADC films to at least reach the "transition" phase. On traversing the PADC film, an alpha particle will leave behind a latent track of damages. Chemical etching will dissolve the damaged region more readily so etching along the latent track will progress at a rate (called the track etch rate V_T) faster that the rate of dissolving the surrounding undamaged bulk material (called the bulk etch rate V_B). The etch pit profile goes through three phases, namely, conical, transition and spherical, as the etching proceeds [30]. At the beginning of the etching, the etchant has not reached the end of the latent track, so the tip of the etch pit remains sharp and the profile of the etch pit remains conical. This phase is referred to as the conical phase. After the etchant has reached the end of the latent track, the etchant will proceed in all directions at the bulk etch velocity V_B so a sphere is now formed around the tip. The upper part of the etch pit is still conical, so the shape of the track has changed to one with a cone joined with a sphere, which will be referred to as "semi-spherical". This phase is called the transition phase. Once a sphere is formed around the tip of the etch pit, i.e., at or beyond the transition phase, the depth of the etch pit will remain constant ever afterwards, since the surface of the PADC film and the bottom of the etch pit will be etched away with the same bulk etch velocity V_B. With further etching, the spherical part is enlarged while the conical part keeps being etched away. If the etching lasts sufficiently long, the conical part will be completely etched away, and

the whole track profile will become and will remain ever afterwards completely spherical. This phase is called the spherical phase.

By choosing to etch the irradiated PADC films to at least reach the transition phase, casts were formed with micrometer-sized pits with the same depth, but with different size and shape. The irradiated PADC films were chemically etched for 14, 18, 22, 26 and 30 h in 6.25 N aqueous NaOH at 70°C giving a bulk etch rate of ~ 1.2 μm/h [31], which was the most commonly employed etching conditions. A separate group of films was unirradiated but etched in exactly the same way as the first group of films (for 14, 18, 22, 26 and 30 h), and were employed as control films. The etched PADC films were glued inside Petri dishes as casts for the substrates.

The 2×2 cm^2 substrates were cast using PDMS (Dow Corning Corporation, Midland, MI). The semi-spherical and spherical pits on the PADC films translated into semi-spherical and spherical pillars protruding from the surface of the PDMS substrate. These substrates were employed for subsequent cell culture. The dimensions of the pits in the PADC films formed by etching in NaOH/H$_2$O, and thus those of the micropillars, could be conveniently calculated using the computer program called TRACK_TEST [32] (also freely available on the webpage: http://www.cityu.edu.hk/ap/nru/test.htm).

2.2 Cell Culture

HeLa cervix cancer cells were obtained from the American Type Culture Collection. HeLa cells were maintained as exponentially growing monolayer at low-passage numbers in Dulbecco's modified eagle medium (D-MEM) supplemented with 10% fetal bovine serum, 1% (v/v) penicillin/streptomycin (Gibco, Germany). The cells were cultured at 37°C in humidified atmosphere containing 5% CO$_2$. Subcultivation was performed every 3–4 days. The cells were trypsinized with 0.5/0.2% (v/v) trypsin/EDTA (ethylene-diamine-tetra-acetic acid; Gibco), and plated out on the 2×2 cm^2 PDMS substrates with different treatments (as described in Sect. 2.1) placed inside a 95 mm diameter Petri dish (adjusted to 3×10^5 cells for each dish). Before cell culture, the PDMS substrates were sterilized by submerging in 75% (v/v) ethyl alcohol for 1 h. After washing with PBS, they were immersed in a fresh medium before cell culture. All cells were allowed to plate out on the PDMS substrates for 3 days.

2.3 EdU (5-ethynyl-2′-deoxyuridine) Assay

Determination of the S-phase index was carried out using Click-iT™ EdU Imaging Kit (Invitrogen, Karlsruhe, Germany) according to the manufacturer's instructions.

Briefly, after 3d culture, the cells were incubated with 10 μM EdU solution at 37°C for 1 h. The cells were then fixed in 2% paraformaldehyde for 20 min and permeabilization was achieved using 0.5% Triton X-100/PBS for 20 min. Subsequently, the fixed cells were incubated with the reaction cocktail containing Alexa Fluor® 488- azide for 30 min and then with 1 μg/ml Hoechst 33342 (for nucleus staining) in PBS for another 5 min. Fluorescent images (magnification: 10×) of cells were captured by a fluorescent microscope (Nikon ECLIPES 80i). The Image-Pro Plus software was used for manually counting the total number of cells (Hoechst 33342) and S-phase cells (Alexa Flour® 488) to determine the percentage of cells in the S-phase in the whole cell population.

2.4 Cell Number

In order to count the cell number attached on the PDMS substrates after 3-day cell culture, the attached cells were released by digestion with trypsin-ethylenediaminetetraacetic acid (Invitrogen) and counted using a hemocytometer (Marienfeld, Germany).

3 Results

3.1 Characterization of Micropillars

The micropillar density on PDMS substrates (equivalently the pit density on the PADC casts) was determined as 213 ± 37 mm^{-2}. By using the program TRACK_TEST [32], the dimensions of tracks with different etching time (14, 18, 22, 26 and 30 h) were determined as shown in Table 1, including the opening diameter $2r$, depth d, aspect ratio ($d/2r$) and profile (phase). The corresponding pillars on the PDMS substrate replicated from the etch pits would thus have a base diameter equal to the track opening-diameter as well as a height equal to the track depth. For simplicity, we will hereafter refer the pillars generated by etching the irradiated PADC films for X h to as X–h micropillars, and the substrates containing the X–h micropillars to as the X–h micropillar substrates. For example, a 14-h micropillar substrate contains 14-h micropillars generated by etching an irradiated PADC film for 14 h.

It is noted here that all pillars had the same height (15.4 μm) due to the fact that chemical etching had reached the transition phase or the spherical phase. The resulting pits were characterized by the spherical tips of the pits [30]. Figure 1 shows the side view of micropillars with different dimensions on a PDMS substrate generated using the program TRACK_TEST [32] (with the pillar produced by 30 h chemical etching being shown as an example to

Table 1 Dimensions of pillars/etch pits produced from different etching time (14, 18, 22, 26 and 30 h), including the pillar base diameter/track-opening diameter 2r, pillar height/track depth d and aspect ratio (d/2r) and profile (phase)

| Etching time (h)	14	18	22	26	30
Opening diameter of track (diameter of pillar base) (μm)	17.7	23.7	30.2	37.1	43.9
Depth of track (height of pillar) (μm)	15.4	15.4	15.4	15.4	15.4
Aspect ratio	0.87	0.65	0.51	0.42	0.35
Profile	Semi-spherical			Nearly spherical	Spherical

incorporate information on the height and base diameter of the pillar from Table 1).

We measured the base diameters of the micropillars from their optical images using the ImageJ software (see Table 2), the heights of the micropillars using VEECO Wyko NT9300 optical surface profiler (see Table 3), and also captured the optical image of the micropillar substrates for examining the profiles (45° tilted; magnification = 100×; see Fig. 2). The dimensions and profiles of the micropillars were commensurate with those given by simulation. Assuming negligible overlapping of pillars, the pillars took up about 5, 9, 15, 23 and 32% of the area of the entire substrate, while the edge areas in which the cells could interact with the pillars were estimated to be about 5, 6, 8, 10 and 14% of the entire substrate, for the 14-, 18-, 22-, 26- and 30-h micropillar substrates, respectively.

Figure 3 shows combined images for HeLa cells with expression of Hoechst 33342 for nucleus staining and with transmission bright field on different PDMS substrates, including the 14-, 18-, 22-, 26- and 30-h micropillar substrates.

3.2 EdU Assay and Cell Number Measurements

A total of 28,203 cells (12,591 and 15,612 cells cultured on control PDMS substrates and micropillar PDMS substrates, respectively) were analyzed for the percentages of cells positively marked by EdU assay. Figure 4 shows the fold changes in the percentage of S-phase cells cultured on different types of PDMS micropillar substrates (corresponding to etching periods of the PADC films from 14 to 30 h with intervals of 4 h), with respect to the cells cultured on the corresponding control PDMS substrates. For example, the percentage of S-phase cells cultured on 14-h micropillar substrates was normalized with that of S-phase cells cultured on control substrates without pillars generated by etching the unirradiated PADC films also for 14 h etching. Although the fold changes for the 18- and 22-h micropillar substrates appeared to be smaller than unity, the differences in the actual percentages for the S-phase cells cultured on the micropillar substrates and the control substrates were not statistically significant
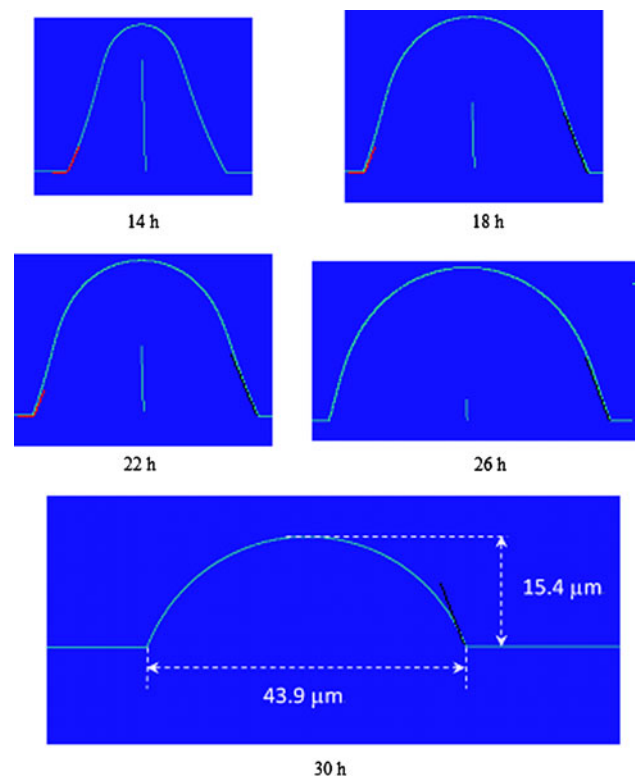
Fig. 1 Simulated side view of micropillars on a PDMS substrate. The pillar produced by 30 h chemical etching was shown as an example to incorporate information on the height (15.4 μm) and base diameter (43.9 μm) of the pillar from Table 1. *The red line* outlined the profile at the base of the 14-h pillar and provided a reference for comparison with those of the 18- and 22-h pillars. *The black line* outlined the profile at the base of the 18-h pillar and provided a reference for comparison with those of the 22-, 26- and 30-h pillars

($p = 0.17$ and 0.08 for 18- and 22-h micropillar substrates, respectively). In contrast, the fold changes for the 14-, 26- and 30-h micropillar substrates were all larger than unity, and the differences in the actual percentages for the S-phase cells cultured on the micropillar substrates and the control substrates were statistically significant ($p = 0.05$, 0.03 and 0.03 for 14-, 26- and 30-h micropillar substrates, respectively). By comparing the effects of different types of pillars, we observed that the normalized percentages of cells in the S-phase were significantly lower for cells cultured on 18- and 22-h micropillar substrates, when

Table 2 Base diameters of the micropillars (95% confidence intervals, CI) measured from their optical images using the ImageJ software, and comparisons with the simulated values

Etching time	14	18	22	26	30
95% CI (μm)	15.6 ± 2.5	25.7 ± 2.4	34.8 ± 2.6	40.9 ± 2.4	41.4 ± 4.2
Simulated value (μm)	17.7	23.7	30.2	37.1	43.9

Table 3 Heights of the micropillars (95% confidence intervals, CI) measured using VEECO Wyko NT9300 optical surface profiler, and comparisons with the simulated values

Etching time	14	18	22	26	30
95% CI (μm)	14.6 ± 2.7	16.3 ± 2.8	15.2 ± 3.5	12.5 ± 2.7	16.9 ± 5.5
Simulated value (μm)	15.4	15.4	15.4	15.4	15.4
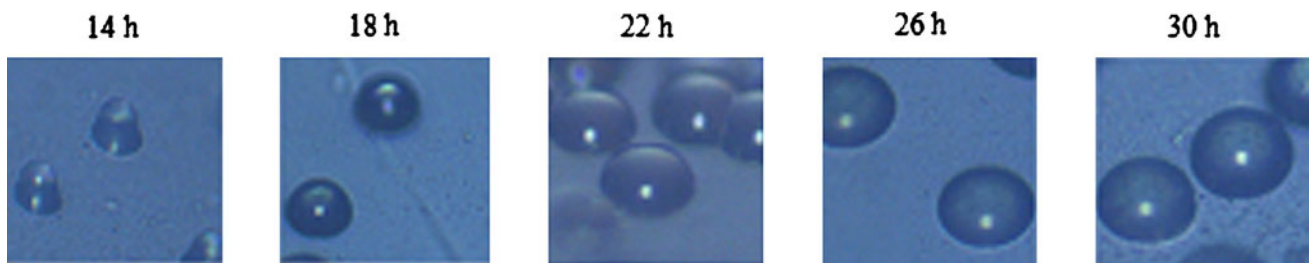
Fig. 2 Optical images of the micropillar substrates (45° tilted; magnification = ×100)

compared to 14-h micropillar substrates ($p < 0.05$ and 0.02), 26-h micropillar substrates ($p < 0.04$ and 0.02) and 30-h micropillar substrates ($p < 0.04$ and 0.02) ($n = 3$).

Figure 5 shows the fold changes in the number of attached cells cultured on different types of PDMS micropillar substrates (corresponding to etching periods of the PADC films from 14 to 30 h with intervals of 4 h), with respect to the cells cultured on the corresponding control PDMS substrates after 3-day cell culture. The normalized number of attached cells were found marginally and significantly higher for 14-h micropillar substrates, when compared to 18-h micropillar substrates ($p = 0.05$) and 22-h micropillar substrates ($p < 0.05$) ($n = 4$). On the other hand, the normalized number of attached cells was significantly lower for 22-h micropillar substrates, when compared to 30-h micropillar substrates ($p < 0.05$) ($n = 4$).

4 Discussion

These substrates were fabricated as replicas of PADC films first irradiated with 5 MeV alpha particles and subsequently etched in NaOH/H$_2$O solution for different periods of time (14, 18, 22, 26 and 30 h). These PDMS micropillar substrates were employed to study the effect of topography on the behavior of HeLa cells through EdU assay and the number of attached cells.

EdU (5-ethynyl-2′-deoxyuridine) is a nucleoside analog to thymidine and is incorporated into DNA during active DNA synthesis (Invitrogen manual MP10338), and it is regarded as an S-phase index. Our results revealed that the normalized percentages of cells in the S-phase were significantly lower for cells cultured on both 18- and 22-h micropillar substrates, when compared with 14-h, 26-h and 30-h micropillar substrates (Fig. 4). This implied comparatively less active proliferation of cells on both 18- and 22-h micropillar substrates and explained our results of a marginally and significantly higher normalized number of attached cells on 14-h micropillar substrates, when compared to 18-h and 22-h micropillar substrates, respectively, after a culture for 3 days. On the other hand, the number of attached cells was significantly lower for 22-h micropillar substrates, when compared to 30-h micropillar substrates (see Fig. 5).

It has been well established that compliance (stiffness/softness) of the ECM can influence cell signaling and the organization of the cytoskeleton to drive changes in cell morphology [33–36]. We propose here that the capability of the cells to mechanosense the curvature of the pillars is a manifestation of a perceived stiffness through compliance mechanosensing. The perceived stiffness is proportional to the ratio between the contractile force and the transverse displacement of the substrate. Whilst attaching to the semi-spherical and the spherical pillars, the cell contractile
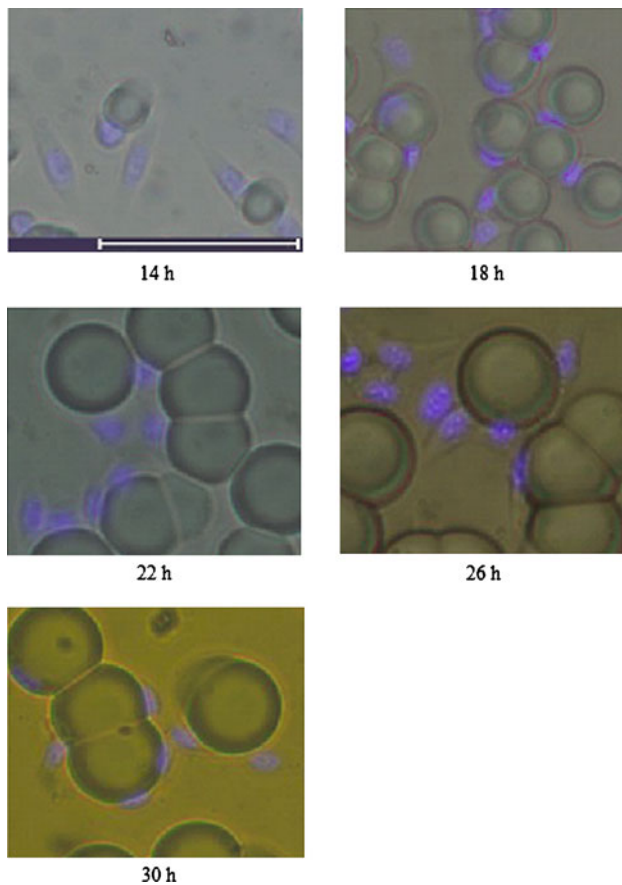
Fig. 3 Combined images for HeLa cells with expression of Hoechst 33342 (*blue*) for nucleus staining and with transmission bright field on different PDMS substrates, including the 14-, 18-, 22-, 26- and 30-h micropillar substrates. *Bar* 100 μm
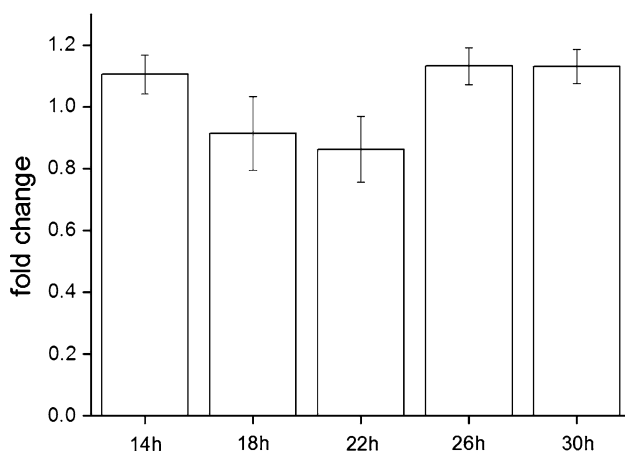
Fig. 4 Fold changes in the normalized percentage of cells in the S-phase for cells cultured on different types of PDMS micropillar substrates, with respect to the cells cultured on the corresponding control PDMS substrates. The normalized percentages of cells in the S-phase were significantly lower for cells cultured on 18- and 22-h micropillar substrates, when compared to 14-h micropillar substrates ($p < 0.05$ and 0.02), 26-h micropillar substrates ($p < 0.04$ and 0.02) and 30-h micropillar substrates ($p < 0.04$ and 0.02) ($n = 3$)
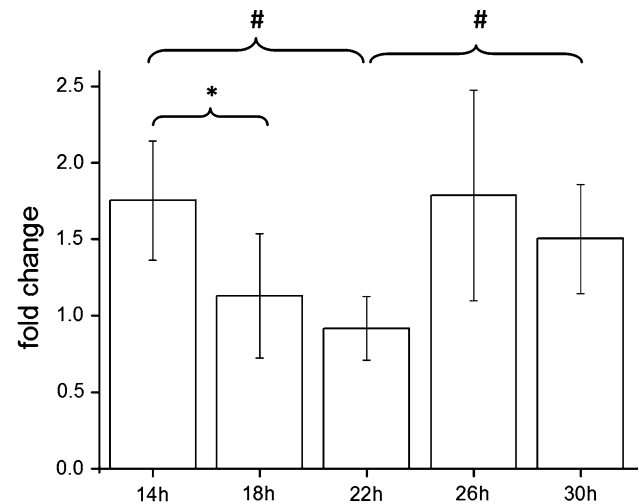
Fig. 5 Fold changes in normalized number of attached cells cultured on different types of PDMS micropillar substrates, with respect to the cells cultured on the corresponding control PDMS substrates after 3-day cell culture. The normalized numbers of attached cells were marginally and significantly higher for 14-h micropillar substrates, compared to 18-h (*$p = 0.05$) and 22-h ($^{#}p < 0.05$) micropillar substrates ($n = 4$), respectively. The normalized numbers of attached cells were significantly lower for 22-h micropillar substrates, compared to 30-h ($^{#}p < 0.05$) micropillar substrates ($n = 4$)

forces were no longer coplanar so that both the shear stress and the corresponding transverse displacement of the substrate would be smaller than those expected for cells on a flat surface (when the forces were coplanar) of the same material with the same shear modulus. Accordingly, the cells would deceptively perceive a less compliant substrate whilst attaching to pillars.

Increase of matrix stiffness was shown to promote cellular proliferation in glioma cells [37]. Schrader et al. [38] also found matrix stiffness regulated epithelial malignancies (Hepatocellular carcinoma) proliferation, in that the cells cultured on stiffer supports had a higher proliferation rate. As such, the enhanced proliferation of HeLa cells cultured on PDMS substrates with micropillars with certain curvature characteristics found in the present work could be explained by their perception of stiffer surfaces. In fact, this idea is also consistent with the report by Rumpler et al. [39] that tissues grew preferentially on surfaces with higher channel curvatures.

Referring to Fig. 1 and Table 1, the pillars in the present work had a uniform height of 15.4 μm which was large compared to the thickness of HeLa cells of ~4 μm [40], and at the same time the pillars had relatively large aspect ratios from 0.35 (30-h pillars) to 0.87 (14-h pillars). Therefore, the HeLa cells were in general attached to the lower parts of the pillars and did not reach the upper parts of the pillars, as evidenced from Fig. 3. As such, the profile of the lower parts of the pillars was the main concern in the present study.

From Figs. 4 and 5, the same trends were observed for the normalized S-phase percentages and cell numbers for different etching time of the PADC films in fabricating the micropillar substrate. Comparing with 18- and 22-h micropillar substrates, the increase in the normalized S-phase percentage was significant for the 14-h micropillar substrates. On the other hand, the increase in the attached cell number on 14-h micropillar substrates was marginally significant over 18-h micropillar substrates and significant over 22-h micropillar substrates.

Referring to Fig. 1 and Table 1, the 14-, 18- and 22-h micropillars were in transition phases. The red line in Fig. 1 outlined the profile at the base of the 14-h pillar and provided a reference for comparison with those of the 18- and 22-h pillars. All these micropillars had a conical lower portion with a similar slope. On the other hand, however, the curvature corresponding to the circumference of the micropillars decreased with increasing etching time of the PADC films, due to the increasing diameter of the pillars. As described earlier, a more curved surface could be deceptively perceived as a stiffer surface by the cells. This explained the higher percentage of cells in S-phase and attached cell number for the HeLa cells cultured on substrates with 14-h micropillars when compared to the substrates with 18- and 22-h ones as shown in Figs. 4 and 5.

On the other hand, according to Figs. 4 and 5, the percentages of cells in the S-phase were significantly higher for cells cultured on both substrates with 26- and 30-h micropillars, when compared to the substrates with 18- and 22-h micropillars. Similarly, the number of attached cells was significantly higher for 30-h micropillar substrates when compared to 22-h micropillar substrates. According to Fig. 1 and Table 1, when the etching time for the irradiated PADC films increased from 18 to 30 h, the profile of the pits changed from semi-spherical (18 and 22 h) to nearly spherical (26 h) and completely spherical (30 h), so the slope of the lower parts of the pillars became progressively curved when the etching time increased. In Fig. 1, the black line outlined the profile at the base of the 18-h pillar and provided a reference for comparison with those of the 22-, 26- and 30-h pillars. Briefly speaking, the 18- and 22-h micropillars had a straight slope, the 26-h micropillars started to have a curved slope, while the 30-h micropillars had prominently curved surface. Accordingly, the stiffness sensed by cells was increased, and so the normalized percentage of cells in S-phase was significantly increased for 26- and 30-h micropillar substrates, when compared to 18- and 22-h micropillar substrates.

The present work employed PADC films as casts to fabricate substrates with micropillars with the same height but with different dimensions and shapes. This novel method provides a whole range of flexibilities in generating substrates with micropillars with different heights and with different characteristics (diameters and shapes), which could be achieved by conveniently varying the incident alpha-particle energies and etching time, with the help of the TRACK_TEST computer program [32].

5 Conclusions

The PDMS micropillars were capable of changing the response of cultured HeLa cells in terms of the percentages of cells in the S-phase and the number of attached cell numbers. Similar trends were observed in the normalized percentages of cells in the S-phase and the attached cell numbers, both of them decreasing from 14-h pillars to 18- and 22-h pillars, and increasing again from 22-h to 26-h and 30-h pillars. The trends could be explained by the mehanosensing of cells in relation to the curvatures provided by different pillars.

References

1. Kaverina I, Krylyshkina O, Small JV (2002) Int J Biochem Cell Biol 34:746
2. Ingber DE (2002) Circ Res 91:877
3. Ghosh K, Thodeti CK, Dudley AC, Mammoto A, Klagsbrun M, Ingber DE (2008) Proc Natl Acad Sci USA 105:11305
4. Mammoto A, Connor KM, Mammoto T, Yung CW, Huh D, Aderman CM, Mostoslavsky G, Smith LE, Ingber DE (2009) Nature 457:1103
5. Fu J, Wang YK, Yang MT, Desai RA, Yu X, Liu Z, Chen CS (2010) Nat Methods 7:733
6. Davidson PM, Fromigue O, Marie PJ, Hasirci V, Reiter G, Anselme KJ (2010) Mater Sci Mater Med 21:939
7. Mussig E, Steinberg T, Schulz S, Spatz JP, Ulmer J, Grabe N, Kohl A, Komposch G, Tomakidi P (2008) Adv Funct Mater 18:2919
8. Steinberg T, Schulz S, Spatz JP, Grabe N, Mussig E, Kohl A, Komposch G, Tomakidi P (2007) Nano Lett 7:287
9. Su WT, Liao YF, Lin CY, Li LT (2010) J Biomed Mater Res A 93A:1463
10. Frey MT, Tsai IY, Russell TP, Hanks SK, Wang YL (2006) Biophys J 90:3774
11. Schulte VA, Diez M, Moller M, Lensen MC (2009) Biomacromolecules 10:2795
12. Ghibaudo M, Trichet L, Le Digabel J, Richert A, Hersen P, Ladoux B (2009) Biophys J 97:357
13. Green AM, Jansen JA, van der Waerden JP, von Recum AF (1994) J Biomed Mater Res 28:647
14. Su WT, Liao YF, Lin CY, Li LT (2010) J Biomed Mate. Res A 15:146
15. Schwarz US, Bischofs IB (2005) Med Eng Phys 27:763
16. Curtis ASG, Varde M (1964) J Natl Cancer Res Inst 33:15
17. Dunn GA, Heath JP (1976) Exp Cell Res 101:1
18. Berry CC, Campbell G, Spadiccino A, Robertson M, Curtis ASG (2004) Biomaterials 25:5781

19. Smeal RM, Rabbitt R, Biran R, Tresco PA (2005) Annals. Biomed Eng 33:376
20. James J, Goluch ED, Hu H, Liu C (2008) Cell Mot Cytos 65:841
21. Rumpler M, Woesz A, Dunlop JWC, van Dongen JT, Fratzl P (2008) J R Soc Interface 5:1173
22. Miller DC, Haberstroh KM, Webster TJ (2005) J Biomed Mater Res A 73:476
23. Rajnicek A, Britland S, McCaig C (1997) J Cell Sci 110:2905
24. Hamilton DW, Wong KS, Brunette DM (2006) Calcif Tissue Int 78:314
25. Berry CC, Campbell G, Spadiccino A, Robertson M, Curtis ASG (2004) Biomaterials 25:5781
26. Su WT (2011) Biomed Microdevices 13:11
27. Baker DW, Liu X, Weng H, Luo C, Tang L (2011) Biomacromolecules 12:997
28. Nematollahi M, Hamilton DW, Jaeger NJ, Brunette DM (2009) J Biomed Mater Res A 91:149
29. Choi CH, Hagvall SH, Wu BM, Dunn JC, Beygui RE, Kim CJ (2007) Biomaterials 28:1672
30. Nikezic D, Yu KN (2004) Mater Sci Eng R Rep 46:51
31. Ho JPY, Yip CWY, Nikezic D, Yu KN (2003) Radiat Meas 36:141
32. Nikezic D, Yu KN (2006) Comput Phys Commun 174:160
33. Pelham RJ Jr, Wang Y (1997) Proc Natl Acad Sci 94:13661
34. Olson MF (2004) Trends Cell Biol 14:111
35. Discher DE, Janmey P, Wang YL (2005) Science 310:1139
36. Saez A, Buguin A, Silberzan P, Ladoux B (2005) Biophys J 89:L52
37. Ulrich TA, de Juan Pardo EM, Kumar S (2009) Cancer Res 69:4167
38. Schrader J, Gordon-Walker TT, Aucott RL, van Deemter M, Quaas A, Walsh S, Benten D, Forbes SJ, Wells RG, Iredale JP (2011) Hepatology 53:1192
39. Rumpler M, Woesz A, Dunlop JWC, van Dongen JT, Fratzl P (2008) J R Soc Interface 5:1173
40. Ng CKM, Wong MYP, Lam RKK, Ho JPY, Yu KN (2011) Radiat Meas 46:1790